Efficient Inclination Control for Geostationary Satellites

D. D. Slavinskas,* H. Dabbaghi,† and W. J. Benden‡
AT&T Bell Laboratories, Holmdel, New Jersey
and
G. K. Johnson§
AT&T-Communications, Hawley, Pennsylvania

Theory and in-orbit experience are presented for an efficient method of inclination control for geostationary satellites. Solar perturbations with a period of six months can cause a stationkeeping fuel consumption overhead that varies between 2.3 and 4.0%. The proposed method controls a component of these perturbations while completely avoiding the fuel penalty. This is equivalent to a service life extension of three to four months for a typical 10 year satellite.

I. Introduction

STATIONKEEPING fuel is a valuable commodity on commercial geostationary satellites because it ultimately limits the revenue-producing life of the spacecraft. Inclination control consumes over 90% of the fuel and, therefore, merits particular attention.

In many applications servicing nontracking ground antennas, inclination is controlled to within 0.05 deg. When various orbit perturbations and orbit prediction errors combine in unison, this tight control can be difficult to guarantee, and an upper limit on the time between maneuvers is imposed. Orbit predictions must account not only for lunisolar secular effects (long-term inclination drift) but also for cyclic (short-term) variations. Expenditure of fuel to compensate for secular drift is unavoidable. Cyclic effects, on the other hand, can, in principle, be either compensated or not. If not compensated, the relatively large solar effect with frequency $2\omega_s$ (period of six months) can add as much as 0.021 deg to maximum inclination excursions. Maximal compensation will reduce the additive cyclic effects, but it will increase the theoretically predicted inclination fuel consumption by 2.3 to 4.0%, depending on the phase of precession of the lunar orbit plane on the ecliptic. Short of resorting to impractically frequent control maneuvers, the choice thus appears to lie between an increase of stationkeeping limits or retainment of these limits at the cost of additional fuel. In practice, the ability to compensate only certain terms may not be available because the orbital software may not be designed for convenient separation of the cyclic terms during inclination maneuver planning.

In this paper we present an inclination control technique that compensates only the component of cyclic terms that is parallel to the direction of secular drift. This approach reduces the cyclic contributions and avoids the 2.3 to 4.0% fuel penalty altogether. The method was conceived and developed jointly by AT&T Bell Laboratories and AT&T-Communications. Under contract with Hughes Aircraft, it has been included in orbital control software and is being used successfully on Telstar 301 at the Hawley, Pennsylvania, Satellite Control Facility.

Presented as Paper 85-0216 at the AIAA 23rd Aerospace Sciences Meeting, Reno, NV, Jan. 14-17, 1985; received May 13, 1985; revision received July 1, 1987.

*Distinguished Member of Technical Staff. Member AIAA.
†Member of Technical Staff.
‡Supervisor, Satellite Engineering Group. Member AIAA.
§Operations Manager, Orbital Dynamics. Member AIAA.

Lunisolar gravitational effects on geostationary orbits are well understood and extensively documented.[1-5] General methods of compensating for these and other perturbations are documented in a definitive paper by Balsam and Anzel.[6] In this paper we consider some specific lunisolar perturbation effects with the aim of achieving fuel-efficient orbit control within small latitude limits.

Inclination can be described in terms of the magnitude h and the right ascension of ascending node Ω, as shown in Fig. 1. Unfortunately, the use of these components leads to singular perturbation equations when h tends to zero. Therefore, in geostationary applications (small h), it is convenient to define the nonsingular components

$$h_1 = h\cos\Omega \tag{1}$$

$$h_2 = h\sin\Omega \tag{2}$$

The latter are shown in Fig. 2 along with unit vectors $\hat{h}_1$ and $\hat{h}_2$. An inclination vector in this notation can be represented by

$$\bar{h} = h(\hat{h}_1\cos\Omega + \hat{h}_2\sin\Omega) \tag{3}$$

We will show later that the motion of the inclination vector is largely represented by the secular component (Fig. 3a) and

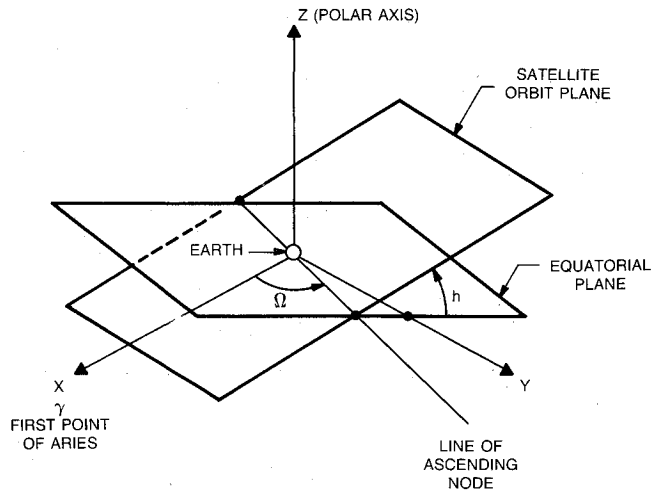

Fig. 1 Orbit inclination parameters h and Ω.

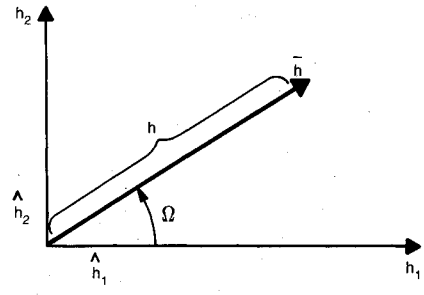

Fig. 2 Inclination vector $\bar{h} = (h_1, h_2)$.

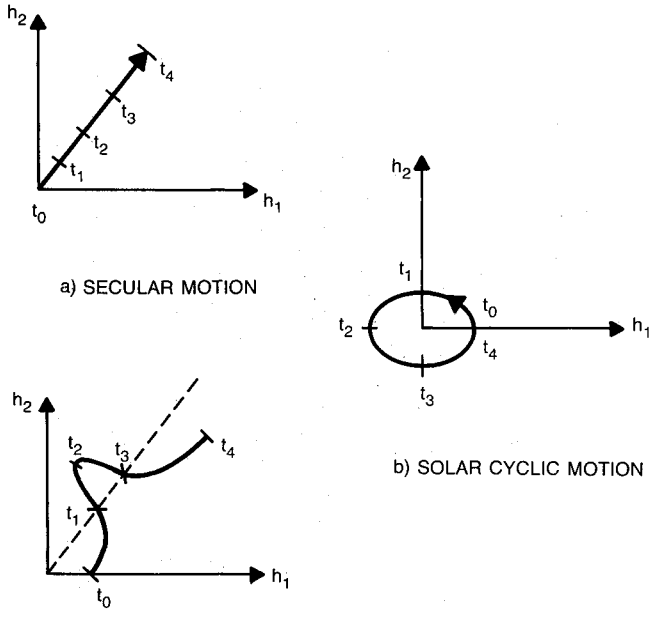

Fig. 3 Secular and cyclic motions.

the solar cyclic component (Fig. 3b). The resultant motion follows the path shown in Fig. 3c, where the time interval from t_0 to t_4 is six months. To compensate for this motion it is necessary to perform periodic impulsive maneuvers, say, every two weeks, of the nature shown in Fig. 4. Assume that at point A the magnitude h has reached the maximum planned value and a maneuver must be performed. In the absence of this maneuver the inclination would drift to point B over the following two weeks. The largest excursion of h is minimized by performing a maneuver Δh such that the midpoint of predicted drift is placed at the orgin. Note that for the small h considered here, the drift vector is independent of the starting point. Therefore, the drift $(D - C)$ is the same as $(B - A)$. The required velocity impulse for the maneuver is approximately proportional to the magnitude $|\Delta \bar{h}|$.

When the maneuver cycle (two weeks) is much shorter than the perturbation cycle (six months), the total impulse requirement over a time interval T_1 to T_2 is approximately proportional to the integral

$$\Delta h(T_1, T_2) = \int_{T_1}^{T_2} |\dot{\bar{h}}| \, dt \tag{4}$$

This is equivalent to the curvilinear distance traced by the evolution of the inclination in the h_1, h_2 plane. Obviously, this distance is greater when the cyclic solar $2\omega_s$ term is included (Fig. 3c) than when it is not (Fig. 3a). The difference varies between 2.3 and 4.0%, depending on the phase of the 18.6 yr lunar orbit precession cycle that affects the direction and rate of secular drift.

The effects of cyclic perturbations are two-fold: 1) they vary the rate of motion along the secular direction, and 2) they displace the inclination vector laterally from the secular direction. Figure 5 illustrates the expected difference in drift of inclination between maneuvers when 1) the cyclic terms are completely uncompensated (not a desirable strategy), and when 2) cyclic terms are compensated in the secular direction but not in the transverse direction. (This method is discussed in the remainder of this paper.)

In the former case, the magnitude h can be considerably larger at one end of the drift cycle than at the other because no longitudinal centering is performed; in the latter case, these magnitudes are more nearly equalized with the result that maximum h is minimized. In the long term, the net fuel used is the same for both cases (proportional to average secular drift).

The following sections address the theory of inclination drift, derive the corresponding velocity impulse requirements, present theoretical inclination excursion limits, discuss details of efficient control implementation, give results of in-orbit experience, and offer final conclusions.

II. Inclination Drift

From previously derived theory,[1-5] the rate of change of inclination averaged over one satellite orbit is well approximated by

$$\langle \dot{\bar{h}} \rangle = \langle \dot{\bar{h}} \rangle_{\text{sun-sec}} + \langle \dot{\bar{h}} \rangle_{\text{moon-sec}} + \langle \dot{\bar{h}} \rangle_{\text{sun-cyc}} + \langle \dot{\bar{h}} \rangle_{\text{moon-cyc}} \tag{5}$$

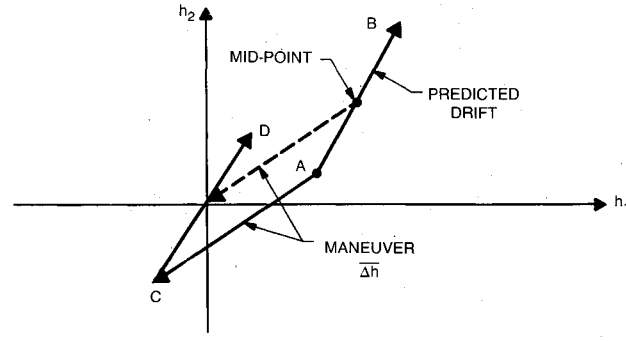

Fig. 4 Maximal correction maneuver.

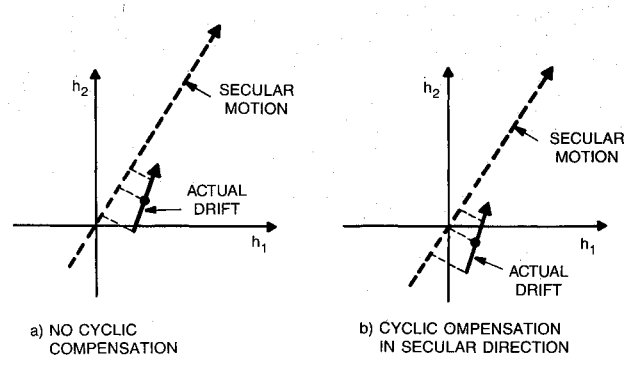

Fig. 5 Effect of cyclic compensation in secular direction.

The solar and lunar secular and periodic terms are given by

$$<\dot{\bar{h}}>_{\text{sun}-\text{sec}} = \frac{3\mu_s}{4nR_s^3}\hat{h}_2 \sin f \cos f \tag{6}$$

$$<\dot{\bar{h}}>_{\text{moon}-\text{sec}} = \frac{3\mu_m}{4nR_m^3}\left\{\frac{1}{2}\hat{h}_1\left[\sin f \sin^2\delta \sin 2\Lambda - \cos f \sin 2\delta \sin\Lambda\right] + \frac{1}{2}\hat{h}_2\left[\sin 2f\left(1-\frac{3}{2}\sin^2\delta\right) + \cos 2f \sin 2\delta \cos\Lambda - \frac{1}{2}\sin 2f \sin^2\delta \cos 2\Lambda\right]\right\} \tag{7}$$

$$<\dot{\bar{h}}>_{\text{sun}-\text{cyc}} = \frac{3\mu_s}{4nR_s^3}\sin f\,(\hat{h}_1 \sin 2\beta_s - \hat{h}_2 \cos f \cos 2\beta_s) \tag{8}$$

$$<\dot{\bar{h}}>_{\text{moon}-\text{cyc}} = \frac{3\mu_m}{4nR_m^3}\left\{\hat{h}_1\left[\frac{1}{2}\left[\sin 2\Lambda \sin f(1+\cos^2\delta) + \sin 2\delta \cos f \sin\Lambda\right]\cos 2\beta_m + \left[\cos\Lambda \sin\delta \cos f + \cos\delta \sin f \cos 2\Lambda\right]\sin 2\beta_m\right] + \hat{h}_2\left[\frac{1}{2}\left[\sin 2f(\sin^2\Lambda - \cos^2\delta\cos^2\Lambda + \sin^2\delta) - \sin 2\delta \cos\Lambda \cos 2f\right]\cos 2\beta_m + \sin\Lambda[\sin 2f \cos\Lambda \cos\delta + \sin\delta \cos 2f]\sin 2\beta_m\right]\right\} \tag{9a}$$

For the last term we will be interested in the case where $\Lambda = 0$ and secular drift is at its maximum (as determined by numerical computations). Thus

$$<\dot{\bar{h}}>_{\text{moon}-\text{cyc}}\Big|_{\Lambda=0} = \frac{3\mu_m}{4nR_m^3}\sin(f+\delta)\left\{\hat{h}_1 \sin 2\beta_m - \hat{h}_2 \cos(f+\delta)\cos 2\beta_m\right\} \tag{9b}$$

The variables are illustrated in Fig. 6 and defined below as follows:

μ_s = solar gravitational constant = 9.9073×10^{20} km^3/day^2
n = sidereal angular rate of the satellite's orbit = 6.3004 rad/day
R_s = mean distance between center of Earth and center of sun = 1.496×10^8 km
f = angle between ecliptic and equatorial planes = 23.441 deg
μ_m = lunar gravitational constant = 3.657×10^{13} km^3/day^2
R_m = mean distance from center of Earth to center of moon = 3.844×10^5 km
δ = angle between ecliptic and lunar orbit planes = 5.1454 deg

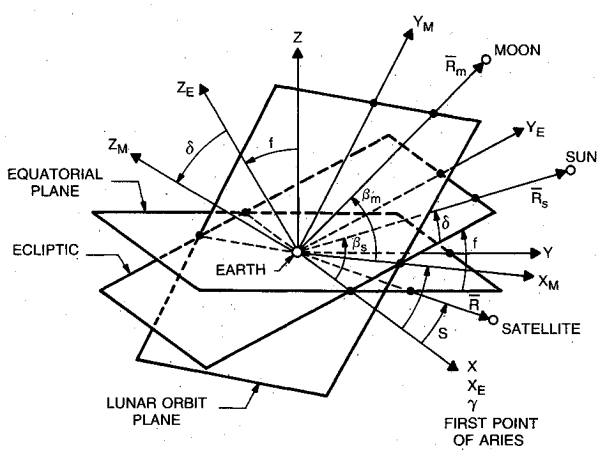

Fig. 6 Coordinate relationships.

Λ = angle from first point of Aries (vernal equinox) to ascending node of the lunar orbit plane on the ecliptic
β_s = angle from first point of Aries to the sun
β_m = angle from ascending node of the moon on the ecliptic to the moon

For the remainder of this century we can use the good approximation[7]

$$\Lambda = 93.913 - 0.0529538t \text{ deg} \tag{10}$$

where t is time in days since Jan 0 at 0 h ET, 1983. For our computational purposes we used a calendar year of 365.25 solar days. The angle of the sun was taken as

$$\beta_s = 360T/365.25 \text{ deg} \tag{11}$$

where T is time in days since the 1983 vernal equinox (March 21).

From the coefficient of Eq. (10), the lunar precession period is given by

$$360/0.05295 = 6799 \text{ days} = 18.6 \text{ yr}$$

Substitution for constants in Eqs. (6–9) yields

$$<\dot{\bar{h}}>_{\text{sun}-\text{sec}} = 0.2691\ \hat{h}_2 \text{ deg/yr} \tag{12}$$

$$<\dot{\bar{h}}>_{\text{moon}-\text{sec}} = \hat{h}_1\,[0.0026 \sin 2\Lambda - 0.1314 \sin\Lambda] + \hat{h}_2[0.5783 + 0.0979 \cos\Lambda - 0.0024 \cos 2\Lambda] \text{ deg/yr} \tag{13}$$

$$<\dot{\bar{h}}>_{\text{sun}-\text{cyc}} = \hat{h}_1[0.2933 \sin 2\beta_s] - \hat{h}_2[0.2691 \cos 2\beta_2] \text{ deg/yr} \tag{14}$$

$$<\dot{\bar{h}}>_{\text{moon}-\text{cyc}}\Big|_{\Lambda=0} = \hat{h}_1[0.7675 \sin 2\beta_m] - \hat{h}_2[0.6739 \cos 2\beta_m] \text{ deg/yr} \tag{15}$$

Equations (12) and (13) establish secular drift rates in the $\hat{h}_1$ and $\hat{h}_2$ directions. It is seen that during the 18.6 yr lunar cycle the rate in the $\hat{h}_1$ direction varies between about -0.13 and $+0.13$ deg/yr. The rate in the $\hat{h}_2$ direction is always positive, varying between 0.75 and 0.94 deg/yr. It is at its highest when Λ is near a multiple of 360 deg. This occurred in 1987 and will occur again in 2006.

Examination of the cyclic rates shows that the motions will describe counterclockwise ellipses in the h_1, h_2 plane.[5] Simple integrations of the rates yield solar cyclic displacement amplitudes of

$$\left.\begin{array}{r} 0.0233 \text{ deg along } h_1, \text{ and} \\ 0.0214 \text{ deg along } h_2 \end{array}\right\} \tag{16}$$

The corresponding lunar amplitudes (for $\Lambda = 0$) are

$$\left.\begin{array}{r} 0.0046 \text{ deg along } h_1, \text{ and} \\ 0.0040 \text{ deg along } h_2 \end{array}\right\} \tag{17}$$

Although the lunar perturbation *rates* are higher than those of the sun, the shorter period (27.3 days vs 1 year) accounts for the much smaller amplitudes of displacements.

III. Impulse Requirements

In this section we determine and tabulate the impulse requirements under various methods of compensation for inclination drift.

Adding the secular terms from Eqs. (12) and (13), we obtain the total secular drift rate

$$<\dot{\bar{h}}>_{\text{sec}} = \hat{h}_1[-0.1314\ \sin\Lambda + 0.0026\ \sin 2\Lambda] + \hat{h}_2[0.8474 + 9.0979\ \cos\Lambda - 0.0024\ \cos 2\Lambda]\ \text{deg/yr} \quad (18)$$

For any time interval (T_1, T_2) the total integrated magnitude of drift is

$$\Delta h_{\text{sec}} = \int_{T_1}^{T_2} \left| <\dot{\bar{h}}>_{\text{sec}} \right| dT \quad (19)$$

The corresponding stationkeeping velocity impulse requirement is well approximated by

$$\Delta V_{\text{sec}} = V_s\left(\frac{\pi}{180}\right)\Delta h_{\text{sec}} \quad (20)$$

where Δh_{sec} is in degrees and V_s is the geosynchronous orbit velocity (10,087 fps).

When the relatively large solar $2\omega_s$ motion is included, the integrated drift becomes

$$\Delta h_{\text{sec+sun-cyc}} = \int_{T_1}^{T_2} \left| <\dot{\bar{h}}>_{\text{sec}} + <\dot{\bar{h}}>_{\text{sun-cyc}} \right| dT \quad (21)$$

Since the cyclic term has a period of six months, integration over multiples of six months will provide meaningful representations of the overhead for including the $2\omega_s$ term. The percent increase due to the cyclic term is

$$P = 100\left[\frac{\Delta h_{\text{sec+sun-cyc}} - \Delta h_{\text{sec}}}{\Delta h_{\text{sec}}}\right] \quad (22)$$

The quantities Δh_{sec}, ΔV_{sec}, and P were evaluated for integration periods of one year and are given in Table 1 for 1984-2004. Note that ΔV_{sec} varies between 132 and 166 fps while P varies between 2.3 and 4.0%. The overhead P is largest when ΔV_{sec} is smallest and vice versa. This penalty in impulse (and thus fuel) requirements is incurred when the standard maximal inclination compensation is exercised. With the presently proposed method of compensating cyclic terms only along the direction of secular drift, the penalty is avoided.

IV. Inclination Excursion Budgets

In this section, we estimate the largest possible inclination excursions when various types of two-week control cycles are used. The analysis presented here assumed circular orbits for the Earth and moon, resulting in perturbations with frequencies $2\omega_s$ and $2\omega_m$. Since the assumption is not strictly true, there are other perturbations at different frequencies. The amplitudes of largest other perturbations[6] are listed in Table 2.

In making the estimates we took the largest secular drift rate along the h_2 axis of 0.9429 deg/yr, which corresponds to a 0.0181 deg displacement in one week. Under this condition the secular drift rate along h_1 is zero. Each perturbation term was phased to produce the largest contribution to inclination magnitude at the ends of the drift cycle. Both methods of summing and root-sum-squaring individual cyclic contributions along h_1 and h_2 were applied. The summed excursions were then converted to inclination magnitude to which we added 0.010 deg to account for orbit determination errors. The latter figure is considered conservative when two-station ranging is used, as was the case in our trial.

Results are given in Table 3. Maximal compensations are superior in control but carry a fuel consumption penalty. Compensation of cyclic terms along the secular drift direction is superior to the no-compensation case, in the sense that it offers better control with no fuel overhead.

V. Implementation

The geometric construction of a partial compensation maneuver (along the secular direction) is shown in Fig. 7. Assume that inclination is predicted to drift from A to B, while the secular drift components along h_1, h_2 are v_1, v_2. Line CD is projected from the midpoint of AB perpendicular to the secular drift line at D. The required maneuver is then given by the vector from D to the origin. If the components of A and B are denoted by a_1, a_2 and b_1, b_2, then the maneuver can be expressed by

$$\Delta\bar{h} = -\frac{1}{2}(\hat{h}_1 v_1 + \hat{h}_2 v_2)\frac{[(a_1 + b_1)v_1 + (a_2 + b_2)v_2]}{(v_1^2 + v_2^2)} \quad (23)$$

Table 1 Inclination compensation requirements

Year	Δh_{sec}, deg	ΔV_{sec}, fps	P solar cyclic overhead, %
1984	0.900	158	2.6
1985	0.920	162	2.5
1986	0.935	165	2.4
1987	0.941	166	2.3
1988	0.943	166	2.3
1989	0.931	164	2.4
1990	0.914	161	2.5
1991	0.890	157	2.6
1992	0.862	152	2.9
1993	0.826	145	3.2
1994	0.794	140	3.5
1995	0.767	135	3.8
1996	0.753	133	4.0
1997	0.748	132	4.0
1998	0.760	134	3.9
1999	0.784	138	3.6
2000	0.817	144	3.3
2001	0.849	149	3.0
2002	0.880	155	2.7
2003	0.907	160	2.5
2004	0.929	164	2.4

Table 2 Nonderived perturbations

Frequency	Amplitude, deg
ω_m	0.0021
ω_s	0.0018
$3\omega_s$	0.0009
$3\omega_m$	0.0007

Table 3 Predicted worst-case inclination excursions in a two-week control cycle

Type of inclination compensation	Maximum excursions, deg: Summed cyclic terms	Maximum excursions, deg: Root-sum-squared cyclic terms	Fuel penalty, %
Maximal	0.038	0.034	2.3-4.0
Partial (cyclic terms along secular direction)	0.050	0.043	0
No cyclic compensation	0.059	0.050	0

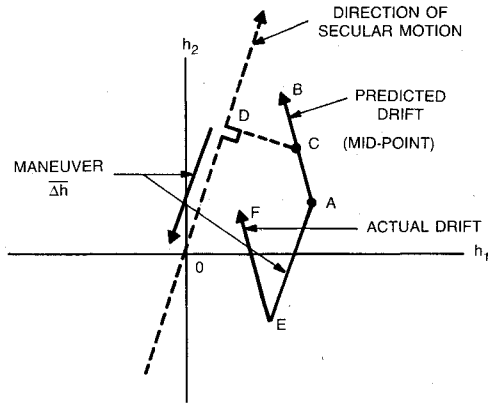

Fig. 7 Construction of partial compensation maneuver.

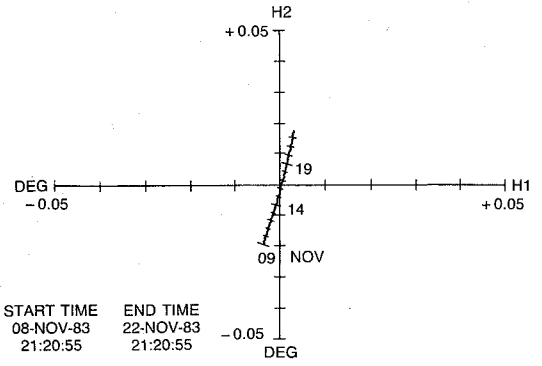

Fig. 8 Inclination drift after initialization.

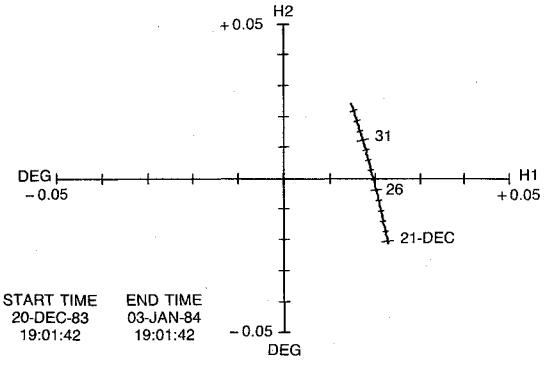

Fig. 9 Inclination drift after third partial compensation.

It should be noted that this maneuver strategy does not exactly equalize the inclination at the start and end of the drift cycle. With some increase in complexity this could be achieved and would yield a reduced maximum inclination excursion by slightly modifying the magnitude of $\Delta\bar{h}$.

The partial compensation method does not control drift components normal to the direction of secular inclination drift. Therefore, the inclination drift over a stationkeeping cycle will be displaced from the previous cycle's drift by an amount proportional to the transverse component of inclination drift. This displacement is cyclic with a period of six months. Because of these excursions, care must be taken to initialize properly the partial correction cycle to center the excursions around the origin in the h_1, h_2 plane.

Several methods are available for proper initialization. The method chosen for Telstar 301 was to carry out a maximal compensation maneuver (with the ensuing drift passing through the origin) near the time when the transverse $2\omega_s$ component is zero. This occurs approximately when the $2\omega_s$ term is changing most rapidly in the h_1 direction, halfway between an equinox and a solstice [see Eqs. (11) and (14)].

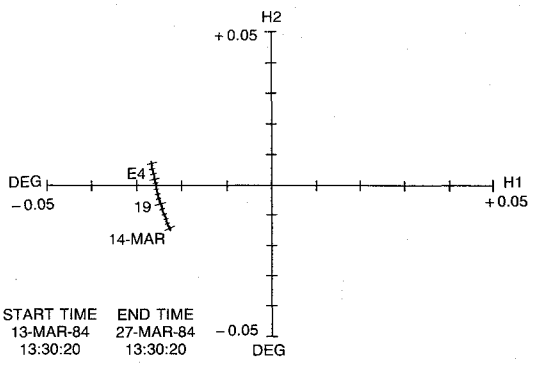

Fig. 10 Inclination drift after ninth partial compensation.

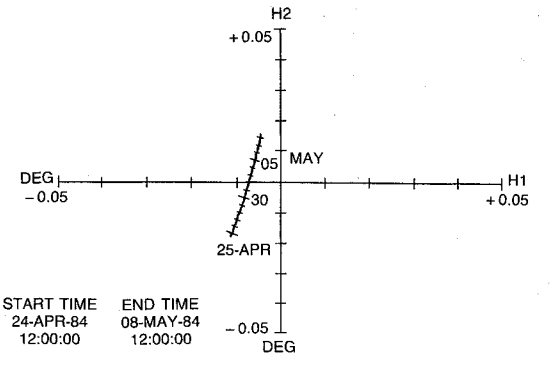

Fig. 11 Inclination drift after twelfth partial compensation.

Telstar 301 was launched July 28, 1983, and after testing was positioned at its assigned station of 96° West longitude by mid-September 1983. At that time normal stationkeeping was established using maximal inclination compensation over a two-week cycle. To determine the best time to begin partial correction maneuvers, simulations were run using orbital operations software.

Four simulations of inclination control cycles (one-half year in length) were conducted using partial compensation after an initial maximum compensation maneuver. Four 1983 dates, bracketing the midpoint between the equinox and solstice were selected as possible starting times: October 11, October 25, November 8, and November 22. Maneuvers were simulated every two weeks, and the maximum latitude excursion after maneuver and the anticipated fuel use for the maneuver were recorded. Results of the latitude excursions are presented in Table 4. Based on that data, it was decided to perform the last total compensation maneuver on November 8, 1983. This date is within a week of the midpoint between the solstice and equinox and has the smallest maximum latitude excursion (0.036 deg) of the four maneuver sets.

VI. Results

On November 8, 1983, the Telstar 301 inclination was corrected using the maximal compensation mode to initialize the cycle for partial compensation maneuvers. Partial compensation maneuvers have been used since that time. Figures 8–11 show plots of predicted mean inclination drift based on the postmaneuver orbit for the initialization maneuvers and the third, ninth, and twelfth partial compensation maneuvers. The mean inclination drift plots do not include short-period (ω_m, $2\omega_m$) terms. The motion shown in Fig. 8, representing inclination after the maximal correction, is typical of conventional stationkeeping methods. The inclination drift for the period is centered about the origin in the h_1, h_2 plane. In this case, inclination goes from a maximum at the start of the cycle, to zero at midcycle, and then back to maximum just

Table 4 Maximum latitude excursions in degrees for various initialization dates

Partial correction cycle	Date of last maximal compensation maneuver			
	Oct. 10, 1983	Oct. 25, 1983	Nov. 8, 1983	Nov. 22, 1983
1	0.023	0.025	0.028	0.024
2	0.032	0.036	0.032	0.028
3	0.044	0.041	0.036	0.024
4	0.048	0.044	0.033	0.023
5	0.051	0.041	0.030	0.020
6	0.049	0.038	0.018	0.029
7	0.045	0.026	0.023	0.035
8	0.033	0.019	0.024	0.040
9	0.024	0.016	0.029	0.039
10	0.014	0.020	0.028	0.034
11	0.016	0.017	0.023	0.025
12	0.014	0.019	0.019	0.022

Table 5 Maximum latitude excursion; simulation vs actual

Partial correction cycle	Actual, deg	Simulation, deg
1	0.026	0.028
2	0.030	0.032
3	0.033	0.036
4	0.029	0.33
5	0.025	0.030
6	0.016	0.018
7	0.022	0.023
8	0.026	0.024
9	0.030	0.029
10	0.029	0.028
11	0.025	0.023
12	0.016	0.019

before the next maneuver. The component of the $2\omega_s$ drift normal to the secular direction is compensated. The motion shown in Figs. 9–11 graphically depicts the effect of partial compensation. There we see that the inclination over the six-month cycle becomes displaced, first in the h_1 direction, and then in the $-h_1$ direction with a return toward the origin.

After each maneuver, checks of maximum latitude excursion and fuel usage were made and compared to those predicted by simulation. Table 5 presents a comparison of expected maximum latitude excursions from the simulation and actual observed data. Agreement is well within the bounds of the 0.01 deg tolerance for orbit and thruster uncertainties. Table 6 presents the comparison of expected fuel usage for maximal and partial corrections (based on simulation) and actual data. As can be seen by reviewing the differences between the simulated and actual data for partial correction, there is a consistently lower fuel consumption shown by the actual data. This difference is on the order of 3% and is near the amount of overperformance that has been noted from the axial thrusters used in these maneuvers. The fuel savings shown for partial correction (actual data) over maximal correction based on simulation are about 6%. After correcting for thruster overperformance, the savings are 3%, which is close to the theoretically expected 2.6% savings during this time period.

Table 6 Maneuver fuel usage (lb): actual vs simulated partial and maximal compensation

Partial correction cycle	Actual, lb	Partial correction simulation, lb	Maximal compensation simulation, lb
1	1.39	1.44	1.44
2	1.56	1.59	1.68
3	1.66	1.68	1.71
4	1.62	1.68	1.70
5	1.55	1.62	1.64
6	1.35	1.44	1.49
7	1.23	1.28	1.33
8	1.04	1.06	1.11
9	1.01[a]	0.98	0.98
10	0.88[b]	0.93	1.05
11	0.98	1.00	1.03
12	1.11	1.11	1.17
Totals:	15.38	15.81	16.33

[a]Maneuver done after 15 days, instead of 14 per simulation. [b]Maneuver done after 13 days, instead of 14 per simulation.

VII. Conclusions

An efficient method of controlling inclination in geostationary applications has been presented analytically and demonstrated by in-orbit experience. The theoretically predicted fuel savings are close to actual results after correction is made for the overperformance of thrusters as compared to estimates prior to launch. For a typical 10 year satellite the 2.3 to 4.0% reduction of fuel consumption can, in the absence of critical component failures, lead to additional revenues worth many millions of dollars.

References

[1]Musen, P., "On the Long-Period Lunar and Solar Effects on the Motion of an Artificial Satellite," *Journal of Geophysical Research*, Vol. 66, Sept. 1961, 2797-2805.

[2]Allen, R.R., "Perturbations of a Geostationary Satellite-2. Lunisolar Effects," Royal Aircraft Establishment, Farnborough, UK, TN Space 47, U.D.C. 629.195.0773: 521.41:521:42, ICSC/T-17 Archives, Sept. 1963.

[3]Allen R.R. and Cook, F.E., "The Long-Period Motion of the Plane of a Distant Circular Orbit," *Proceedings of the Royal Society of London, Ser. A, Mathematical and Physical Sciences*, Vol. 280, July 1964, 97-109.

[4]Frick, R.H., "Orbital Regression of Synchronous Satellites due to the Combined Gravitational Effects of the Sun, the Moon and the Oblate Earth," NTIS, U.S. Dept. of Commerce, R-454-NASA, Aug. 1967.

[5]Kamel, A. and Tibbitts, R. "Some Useful Results on Initial Node Locations for Near-Equatorial Circular Satellite Orbits," *Celestial Mechanics*, Vol. 8, Aug. 1973, pp. 45–73, 1973.

[6]Balsam, R.E. and Anzel, B.M., "A Simplified Approach to Correction of Perturbations on a Stationary Orbit," *Journal of Spacecraft and Rockets*, Vol. 6, July 1969, pp. 805–811.

[7]*The Astronomical Almanac*, U.S. Government Printing Office, 1983.